

Article

Open Access



# *In-situ* polymerized and crosslinked electrolytes with interchangeable Li/Na transport for battery applications

Harmandeep Singh<sup>1</sup>, Josh T. Damron<sup>2</sup>, M Shahriar<sup>3,4</sup>, Mary Danielson<sup>2</sup>, Rob Beard<sup>2</sup>, Rachel Eberhard<sup>2</sup>, Georgios Polizos<sup>3</sup>, Ivan Popov<sup>5</sup>, Md Anisur Rahman<sup>2,\*</sup>, Alexei P. Sokolov<sup>2,6</sup>, Catalin Gainaru<sup>2,\*</sup>

<sup>1</sup>Bredesen Center for Interdisciplinary Research and Graduate Education, University of Tennessee, Knoxville, TN 37996, USA.

<sup>2</sup>Chemical Sciences Division, Oak Ridge National Laboratory, Oak Ridge, TN 37831, USA.

<sup>3</sup>Electrification and Energy Infrastructures Division, Oak Ridge National Laboratory, Oak Ridge, TN 37831, USA.

<sup>4</sup>Department of Mechanical Engineering, Iowa State University, Iowa, IA 50010, USA.

<sup>5</sup>University of Tennessee - Oak Ridge Innovation Institute, University of Tennessee, Knoxville, TN 37996, USA.

<sup>6</sup>Department of Chemistry, University of Tennessee, Knoxville, TN 37996, USA.

\*Correspondence to: Dr. Md Anisur Rahman and Dr. Catalin Gainaru, Chemical Sciences Division, Oak Ridge National Laboratory, Oak Ridge, TN 37831, USA. E-mail rahmana1@ornl.gov; gainarucp@ornl.gov

**How to cite this article:** Singh, H.; Damron, J. T.; Shahriar, M.; Danielson, M.; Beard, R.; Eberhard, R.; Polizos, G.; Popov, I.; Rahman, M. A.; Sokolov, A. P.; Gainaru, C. *In-situ* polymerized and crosslinked electrolytes with interchangeable Li/Na transport for battery applications. *Energy Mater.* **2025**, *5*, 500149. <https://dx.doi.org/10.20517/energymater.2025.07>

**Received:** 12 Jan 2025 **First Decision:** 4 Mar 2025 **Revised:** 6 Mar 2025 **Accepted:** 11 Mar 2025 **Published:** 30 Sep 2025

**Academic Editors:** Jose Antonio Alonso, Federico Bella **Copy Editor:** Ping Zhang **Production Editor:** Ping Zhang

## Abstract

The next generation of batteries requires electrolytes with high conductivity, mechanical stability, good adhesion with electrodes, wide electrochemical windows, and scalability. The present study introduces a concept of doped quasi single-ion conducting copolymers based on methacrylate-(trifluoromethanesulfonyl)imide (TFSI) and vinyl ethylene carbonate which at room temperature are mechanically robust and display ionic conductivities of ~0.1 mS/cm. These electrolytes can be polymerized/crosslinked *in-situ*, making them easily implementable in current battery manufacturing technologies. They also allow for switching between Li<sup>+</sup> and Na<sup>+</sup> transport using simple chemistry procedures. To demonstrate their potential for battery applications, the newly developed Li conductors have been tested in symmetric cells, exhibiting overall impedance below 350 Ohm and plating/stripping stability up to 1 mA/cm<sup>2</sup>. Moreover, lithium metal batteries incorporating this electrolyte and high-voltage Lithium Nickel Manganese Cobalt Oxide (NMC) cathodes show good capacity retention (~79%) during charging and discharging for 80 cycles at C/10 rate and a Coulombic efficiency close to 100% in the entire measurement range. The compositional, mechanical and electrochemical versatility of these electrolytes opens new venues for the design of polymer-based batteries capable of fast charging and extended cycle life, aligning with the current global green



© The Author(s) 2025. **Open Access** This article is licensed under a Creative Commons Attribution 4.0 International License (<https://creativecommons.org/licenses/by/4.0/>), which permits unrestricted use, sharing, adaptation, distribution and reproduction in any medium or format, for any purpose, even commercially, as long as you give appropriate credit to the original author(s) and the source, provide a link to the Creative Commons license, and indicate if changes were made.



energy storage strategies.

**Keywords:** Polymer electrolytes, ion transport, electrochemical performance, batteries

## INTRODUCTION

The surging demand for safe, high-energy density storage in household appliances, mobile electronics and electric vehicles calls for new strategies in mitigating current limitations of liquid electrolyte-based batteries<sup>[1,2]</sup>. Most ceramic electrolytes, despite their high  $\text{Li}^+/\text{Na}^+$  conductivities and large mechanical stiffnesses<sup>[3]</sup>, suffer from electrochemical instability, poor electrode contact, inability to suppress dendrite formation, and deficient large-area manufacturing<sup>[4]</sup>. While polymer electrolytes such as salt-doped poly(ethylene oxide) (PEO) and their ceramic composites provide a good alternative in terms of mechanical flexibility, electrode adhesion, and processability<sup>[5-7]</sup>, they often display relatively low room temperature conductivity and limited electrochemical window<sup>[8-10]</sup>.

Combining high charge density of ionic liquids with safety and operational stability of nonfluid electrolytes, single-ion conducting polymers (SICPs)<sup>[11-13]</sup> can overcome many technological drawbacks of ceramics and salt-doped polymers<sup>[14,15]</sup>. These polymers can be produced in a wide morphological diversity, allow roll-to-roll manufacturing, and their ability to incorporate transient bonds opens exciting possibilities for energy storage in 3D-printed<sup>[16]</sup> or self-healing batteries<sup>[17]</sup>. In most SICPs, all anions are covalently attached to the polymer chains, generating a negatively charged, solid-like matrix in which the cations (e.g.,  $\text{Li}^+/\text{Na}^+$ ) can perform long-range diffusion. With the anion species effectively immobilized, the SICPs are characterized by large cation transport numbers  $t_+$  close to 1<sup>[18]</sup>, at variance with the salt-doped polymer electrolytes for which  $t_+ \sim 0.05-0.3$ <sup>[19-21]</sup>. A high  $t_+$  is critical for the battery performance because it reduces its polarization, enabling high charge/discharge rates. Moreover, attaching the anions to chains is beneficial for achieving a homogeneous distribution of charge carriers at the electrodes. Recent theoretical and experimental works demonstrated that dendrite growth can be more efficiently suppressed by creating such uniformly charged interfaces<sup>[22,23]</sup>, rather than employing high mechanical strength electrolytes but with inhomogeneous structures<sup>[24]</sup>.

Despite these many advantages, the deployment of bulk SICPs for battery applications is hampered by their relatively low conductivity near ambient temperature<sup>[25]</sup> and by their faulty (solid-solid) adhesion to the porous cathode material<sup>[26]</sup>. Salt doping can be a solution to the first issue<sup>[27]</sup>, as long as the cation transport number does not drop significantly below 0.5. Regarding the second issue, a uniform, low impedance electrolyte-electrode interface (EEI) is required for good battery performance<sup>[28]</sup>. In traditional batteries, liquid electrolytes penetrate porous electrodes, forming smooth EEI that facilitates cation transport from the electrolyte to the electrode<sup>[1,29]</sup>. In this regard, *in-situ* polymerization of SICPs has recently gained increased popularity<sup>[30-32]</sup>. The main idea of this approach is that the initial liquid monomer precursor fills in all the pores and forms good contact with electrodes in the assembled cell, and then the electrolyte progressively increases its mechanical strength in direct contact with the electrodes during polymerization upon heating. This technique provides homogeneous electric contact and strong adhesion between the SICP and the electrodes, preventing nucleation and growth of Li dendrites during cycling even at relatively high current densities<sup>[33]</sup>.

Based on the above considerations, in our previous study we introduced an electrolyte concept based on a quasi-SICP obtained via *in-situ* copolymerization of lithium (4-styrenesulfonyl) (trifluoromethanesulfonyl) imide (LiSTFSI, a monomer of a “classical”  $\text{Li}^+$  SICP) and vinyl ethylene carbonate (VEC), in the presence of

Li-TFSI salt and thermal initiators<sup>[32]</sup>. The proposed concept was built on several fundamental ideas: polymerized anions increase  $t_+$ ; *in-situ* polymerization enables homogeneous contact with electrodes; high polarity of VEC units decreases the strength of electrostatic interactions<sup>[34]</sup> for achieving high  $\text{Li}^+$  mobility; and small amounts of non-polymerized small-molecule precursors and salt enable high ambient ionic conductivity, while preserving relatively high  $t_+$ . Several preliminary tests demonstrated the feasibility of this electrolyte concept in Li symmetric- and high-voltage cell configurations<sup>[32]</sup>.

Despite these benefits, the above-mentioned prototypic material presented several technological drawbacks: (i) it was not crosslinked and contained a significant amount of unpolymerized monomers; its reduced viscosity posed substantial safety concerns; (ii) the polymerization of styrene units required relatively long time, which is a major drawback for energy efficient scalability, and (iii) it was not fully optimized for compliance with high-voltage electrodes [e.g., Lithium Nickel Manganese Cobalt Oxide (NMC)-based] as required for high energy batteries. The present work continues the development of this polymer electrolyte concept to include *in-situ* crosslinking in addition to polymerization for increasing the mechanical robustness of the material to the level of a solid-like, free-standing film at ambient conditions. In addition, to significantly shorten the polymerization process, we replaced the precursor solution styrene-TFSI<sup>-</sup> with methacrylate-TFSI<sup>-</sup> (MTFSI)<sup>[35]</sup>. Moreover, we demonstrate that the same electrolyte can be used for  $\text{Na}^+$ -based systems.

While the concept of *in-situ* polymerized polymer electrolytes has been explored in previous studies, in our work we advance this approach by incorporating *in-situ* crosslinking of VEC and Lithium 1-[3-(methacryloyloxy)propylsulfonyl]-1-(trifluoromethylsulfonyl) imide (LiMTFSI)/Sodium 1-[3-(methacryloyloxy)propylsulfonyl]-1-(trifluoromethylsulfonyl) imide (NaMTFSI) monomers with a Trimethylolpropane triacrylate (TTA) to develop a more robust and mechanically stable polymer electrolyte system. This strategy enhances the electrolyte's structural integrity, ion transport, and overall performance. Our new results demonstrate that this optimization reduces the polymerization time by a factor of 3 without compromising the high conductivity level of the electrolyte. The batteries assembled with these newly developed *in-situ* polymerized/crosslinked copolymers demonstrate cycling stability of up to 1 mA/cm<sup>2</sup> in  $\text{Li}^+/\text{Li}$  symmetric cells and good compatibility with high-voltage NMC-type cathodes. A major advantage of (single- or dual-ion conducting) polymers over ceramics is that by relatively simple chemical procedures, one can adapt the composition for various types of mobile cations. This extends the applicability range of the proposed concept into the “beyond Li” habitat scrutinized by recent battery studies<sup>[36-39]</sup>. In this regard, the newly introduced  $\text{Na}^+$  electrolyte displays similar properties as its  $\text{Li}^+$  counterpart, including mechanical robustness and conductivities of ~0.1 mS/cm at room temperature. The present results and analysis complement several recent studies that demonstrate the high potential of polymeric materials as solid-state or quasi-solid-state electrolytes for energy storage applications<sup>[32,40-43]</sup>.

## EXPERIMENTAL

### Materials and Synthesis

#### Materials

LiMTFSI and NaMTFSI were purchased from Specific Polymers. Lithium bis(trifluoromethanesulfonyl)imide (LiTFSI), Sodium bis(trifluoromethanesulfonyl)imide (NaTFSI), VEC, azodiisobutyronitrile (AIBN), and TTA and dimethyl carbonate (DMC) were purchased from Sigma Aldrich. TTA has been passed through an aluminum oxide/inhibitor remover-loaded column to remove the inhibitor. AIBN was recrystallized from methanol before use.

### *Synthesis of poly(VEC-r-LiMTFSI)*

The VEC (2 g, 17.5 mmol), LiMTFSI (~0.604 g, 1.75 mmol), and LiTFSI (0.5 g) were taken in a glass bottle and stirred for 30 min to form a homogeneous solution. The AIBN (28 mg, 0.171 mmol) as the initiator was added to the solution and stirred for ~30 min, yielding a clear precursor solution. The resulting solution was polymerized under an inert atmosphere at 75 °C for 2-3 h to form a gel-type polyelectrolyte [Scheme 1].

### *Synthesis of crosslinked Li- polyelectrolyte*

A similar polymerization procedure was used to synthesize *in-situ* crosslinked poly-electrolyte gel [Scheme 2]. The VEC (2 g, 17.5 mmol), LiMTFSI (~0.604 g, 1.75 mmol), and LiTFSI (0.5 g) were taken in a glass bottle and stirred for 30 min to form a homogeneous solution. The crosslinker TTA (0.047 g, 0.16 mmol) was added to the solution. AIBN (28 mg, 0.171 mmol) was then added as an initiator, and the mixture was stirred for approximately 30 minutes, yielding a clear precursor solution. The resulting precursor solution was polymerized under an inert atmosphere at 75 °C for 2-3 h, forming a gel-type crosslinked polyelectrolyte.

### *Synthesis of crosslinked Na-polyelectrolyte*

A similar polymerization procedure was used to synthesize *in-situ* crosslinked sodium (Na)-based poly-electrolyte gel [Scheme 3]. The VEC (2 g, 17.5 mmol), NaMTFSI (~0.634 g, 1.75 mmol), and NaTFSI (0.532 g, 1.75 mmol) were put in a glass bottle and stirred for 30 min to form a homogeneous solution. The crosslinker TTA (0.047 g, 0.16 mmol) was added to the solution. AIBN (28 mg, 0.171 mmol) was then added as an initiator, and the mixture was stirred for approximately 30 minutes, yielding a clear precursor solution. The resulting precursor solution was polymerized under an inert atmosphere at 75 °C for 2-3 h, forming a gel-type crosslinked polyelectrolyte.

### *Broadband dielectric spectroscopy*

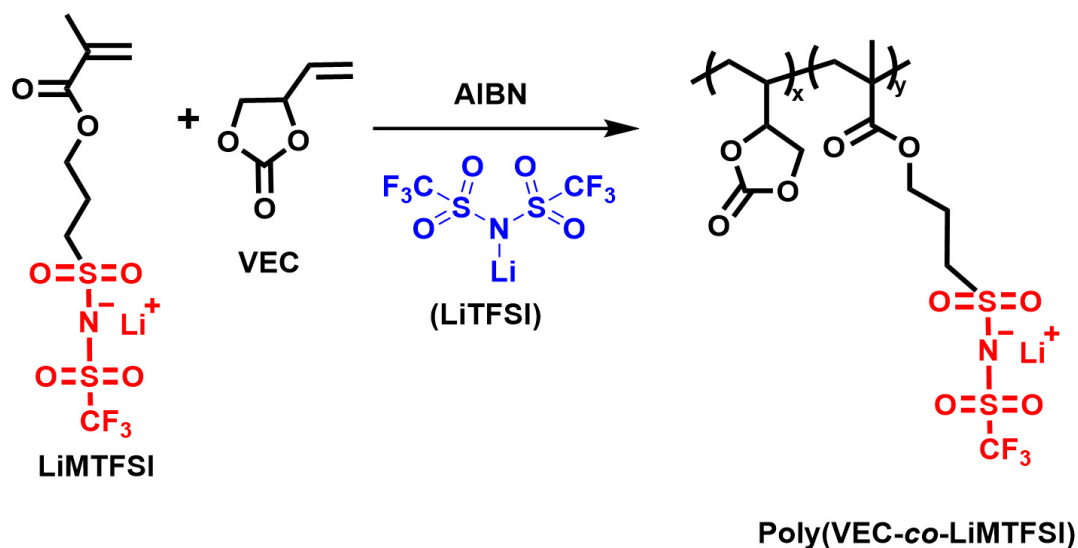
The conductivity response of the newly introduced electrolytes was probed in a frequency range covering  $10^{-2}$ - $10^6$  Hz with a 0.1 V voltage amplitude using an Alpha-A analyzer from Novocontrol. A Quattro temperature controller (also from Novocontrol) was used to achieve a temperature stabilization of the samples within  $\pm 0.2$  K. The dielectric capacitor consisted of two electrodes with a diameter of 10.2 mm and separated by means of a sapphire disk at a fixed distance of 0.4 mm.

### *Pulse field gradient nuclear magnetic resonance*

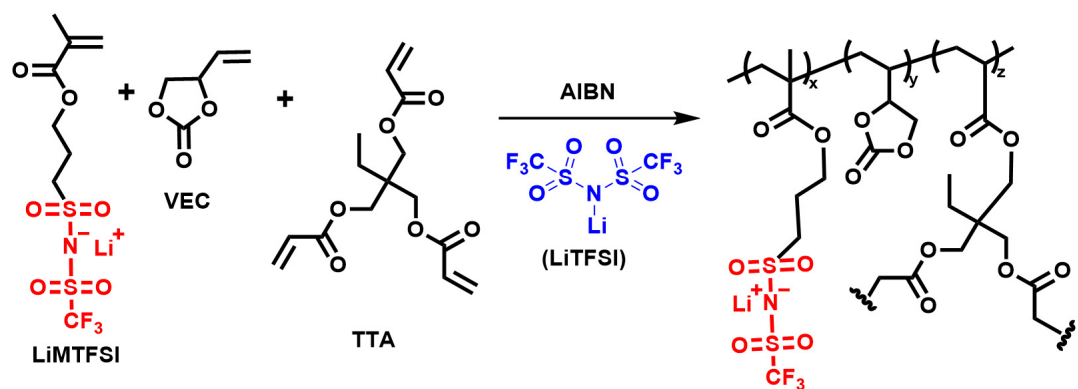
Pulse Field Gradient Nuclear Magnetic Resonance (PFG-NMR) experiments were performed on a 400 MHz Bruker NEO spectrometer equipped with a diff50  $^1\text{H}/\text{X}$  diffusion probe using a stimulated echo with bipolar gradient pulses ranging from 2-2.5 ms and a diffusion delay of 200 ms. Variable temperature experiments were performed using a BCU II and the samples were allowed to equilibrate for 5 min before each measurement.

### *Battery testing*

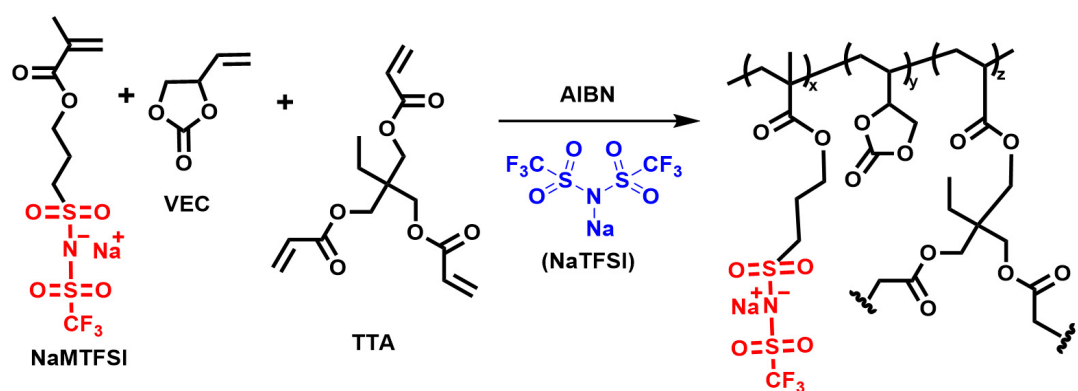
The electrolyte precursor and the AIBN initiator were mixed inside an Argon-filled glove box. The solution was cast onto the cathodes and CR2032 coin cells were assembled using lithium metal for the anode. Prior to testing, the cells were annealed at 60 °C overnight to allow polymerization and crosslinking of the electrolyte monomers. The electrochemical long-term cycling testing was performed at 30 °C on a Maccor battery cycler (series 4000) at a C/10 rate. The cutoff voltage was 2.5 and 4.2 V for the Lithium Iron Phosphate (LFP)-based cell and 3 and 4.2 V for NMC622-based cells. Electrochemical impedance spectra (EIS) were conducted on a BioLogic VSP3 potentiostat at an amplitude of 10 mV. The frequency range was from 1 MHz to 10 mHz. The EIS and cyclic voltammetry (CV) measurements were performed on a full-cell



Scheme 1. Synthesis of poly(VEC-r-LiMTFSI) via free radical polymerization.



Scheme 2. Synthesis of crosslinked Li- polyelectrolyte via free radical crosslinking.



Scheme 3. Synthesis of crosslinked Na- polyelectrolyte via free radical crosslinking.

configuration with a lithium metal anode. The cathode formulation was based on 90 wt% active material, 5 wt% carbon black, and 5 wt% polyvinylidene fluoride binder. The active material loading was 2.8 mg/cm<sup>2</sup>

for the LFP-based cell and 2.19 mg/cm<sup>2</sup> for the NMC622-based cells. Plating/stripping at several current densities and transference number experiments were carried out on Li symmetric cells (12 mm in diameter). The transference number calculations were performed according to the Bruce-Vincent method by applying 5 mV for 2 h. The electrospun Polyacrylonitrile (PAN) separator was approximately 30  $\mu$ m thick.

## RESULTS AND DISCUSSION

### Transport properties of the proposed electrolytes

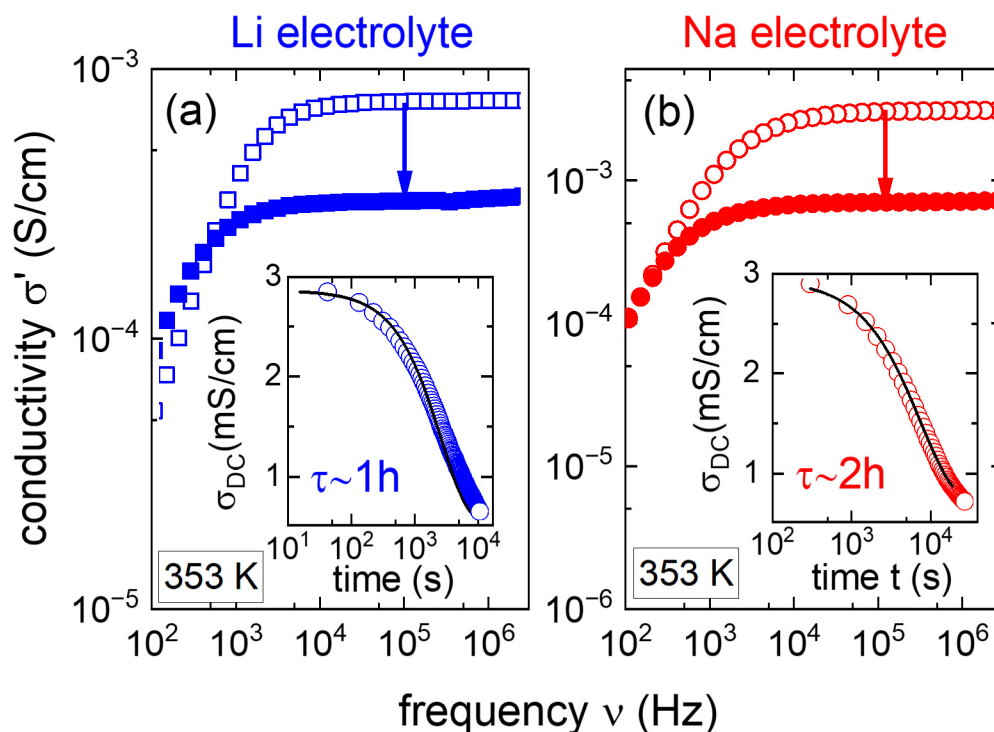
The “final” electrolyte products (after thermally-induced free radical polymerization/crosslinking) are random copolymers including MTFSI<sup>-</sup> and VEC monomers, which incorporate unpolymerized VEC fragments and mobile ions. According to proton NMR data [Supplementary Figure 1], while all LiMTFSI monomers were fully polymerized, only 40% of the VEC monomers underwent polymerization. The remaining unreacted VEC monomers function as plasticizers, increasing the conductivity. The mechanism of conductivity in our gel-like electrolyte resembles that in liquid electrolytes - strongly coupled to structural relaxation of the matrix, i.e., similar to doped PEO<sup>[20]</sup>. However, due to the significant number of anions attached to the chain, the transport number is higher than in PEO electrolytes<sup>[21]</sup>. The relative amount of freely migrating cations is controlled by the relative concentrations of MTFSI<sup>-</sup> present in the matrix and of the doping salt (LiTFSI or NaTFSI). Considering this morphological complexity, our initial tests focused on the Li-based material for determining which [VEC]:[MTFSI]:[LiTFSI] composition provides the highest conductivity near room temperature. To this end, we performed temperature-dependent conductivity measurements on several electrolytes with different relative concentrations of these three components. We followed the *in-situ* polymerization (at 80 °C, overnight) of these samples with and without crosslinkers directly in the probing capacitor. Based on these results [Supplementary Figure 2], a [VEC]:[MTFSI]:[LiTFSI]=100:10:10 molar composition has been chosen for the battery tests due to its balanced high conductivity and mechanical strength. For facilitating comparison, the same ratio [VEC]:[MTFSI]:[NaTFSI]=100:10:10 has also been chosen for the Na electrolyte.

Figure 1 presents the time evolution of several selected conductivity responses recorded during the *in-situ* polymerization/crosslinking performed at 80 °C for the (100:10:10) Li and Na electrolytes. These spectra display at high frequencies the direct current (DC) conductivity plateaus with amplitudes  $\sigma_{DC}$ <sup>[44]</sup>, while at low frequencies, they reflect polarization effects due to ion blocking at the electrodes<sup>[45]</sup>. As indicated by the two arrows, polymerization/crosslinking of electrolytes triggers a progressive decrease of their DC conductivities below the  $3 \times 10^{-3}$  S/cm value corresponding to both precursors at 80 °C (the short-time  $\sigma_0$  value in inset Figure 1).

To parameterize the time evolutions of  $\sigma_{DC}$ , we performed interpolations of the data presented in the two insets of Figure 1 with exponential decay functions  $F(t) \propto \exp[-(t/\tau)]$  providing the characteristic times  $\tau$  of polymerization/crosslinking kinetics. These functions provided relatively good interpolation of experimental data with  $\tau$  close to one hour for the Li system and two hours for the Na counterpart. These time constants are logistically relevant, since they can guide the optimization of polymerization/crosslinking inside the batteries. Based on our results, for the presently introduced methacrylate-based Li electrolyte, at 80 °C, this process can be considered effectively completed after  $(4-5 \times \tau) \sim 4-5$  h. However, the polymerization of methacrylate-based Na electrolytes requires eight to ten hours, and further optimization of its composition could reduce this time.

After the isothermal polymerization/crosslinking of the two electrolytes, their frequency-dependent conductivity response were probed over a temperature range from 80 °C down to -65 °C. These spectra are shown in Supplementary Figure 3 and have been used for extracting the DC conductivities plotted as a





**Figure 1.** Selected spectra illustrating the evolution of the conductivity response during the polymerization/ crosslinking process induced at 80 °C for (A) Li electrolyte and (B) Na electrolyte. The two insets present the corresponding time evolution of  $\sigma_0$  for the two materials. The solid lines represent fits using exponential decay functions.

function of the inverse temperature in Figure 2. Here, the presently considered electrolytes are denoted as “copolymers with salt”.

Figure 2 shows that both Li and Na polymer-based electrolytes display similar conductivities in their common investigated  $T$  range. Accordingly, replacing MTFSI-Li with MTFSI-Na monomers and LiTFSI with NaTFSI salt is not detrimental in terms of conductivity. These results demonstrate the versatility of the present concept for enabling fast transport for different types of cations. According to Figure 2, the conductivity of the two doped copolymers near room temperature is about 0.1 mS/cm, which is quite high for mechanically robust electrolytes. To put these results in a broader perspective, we included in Figure 2 the  $\sigma_{DC}$  results corresponding to the same copolymers without salt (from this work, composition 100:10:0 according to the present nomenclature) and for MTFSI-Li/MTFSI-Na homopolymers, with no VEC and no salt (literature data<sup>[46]</sup> composition 0:100:0). The latter materials are the SICPs with the largest concentration of free  $\text{Li}^+$ /  $\text{Na}^+$  ions, however, due to their high glass transition temperatures ( $T_g > 450$  K)<sup>[46]</sup>, their ambient conductivities are very low. With corresponding  $\sigma_{DC}$  below  $10^{-13}$  S/cm near room temperature, these homopolymers have no practical relevance for battery applications.

However, this situation changes when a large amount of mTFSI monomers are “replaced” with the VEC ones forming a copolymer without salt. As recognized in Figure 2, despite having a significantly lower number density of cations, these materials - which are still SICPs - display room-temperature  $\sigma_{DC}$  values close to  $10^{-5}$  S/cm (for Li). This strong increase in conductivity occurs due to VEC acting both as a good plasticizer, strongly reducing the glass transition of the polymer, and as a highly polar group screening the Coulombic interaction. To further increase  $\sigma_{DC}$  to about  $10^{-4}$  S/cm, these copolymers are doped with a certain

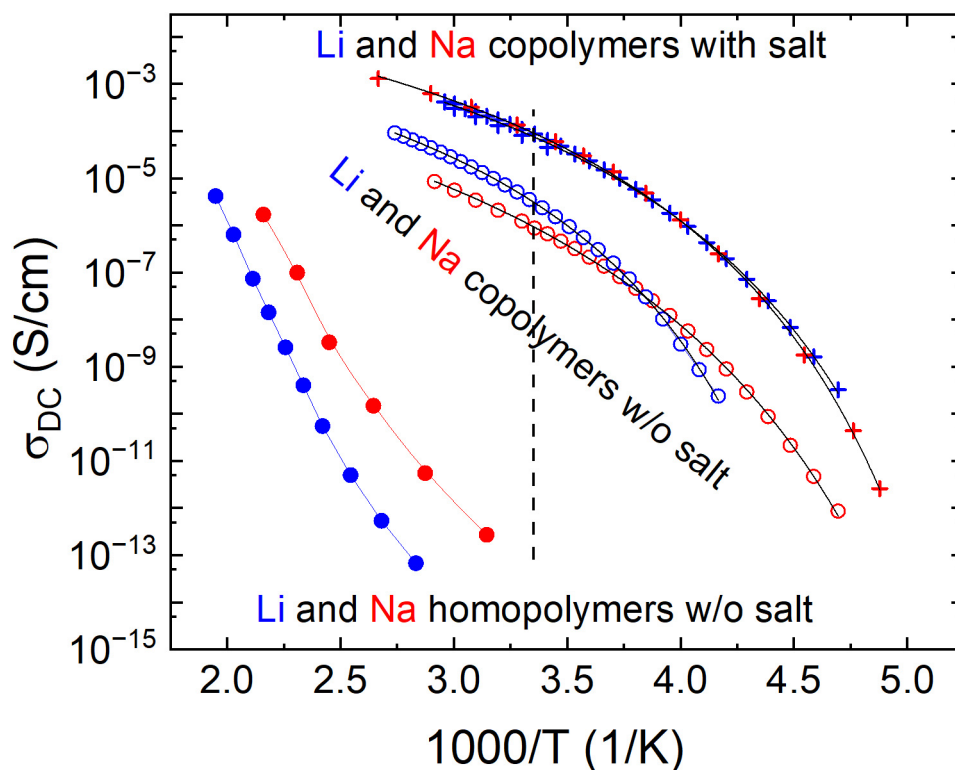


**Figure 2.** Comparison of DC conductivities corresponding to Li (blue symbols) and Na (red symbols) homopolymers (dots), copolymers without salt (open circles), and copolymers with salt (crosses); see text for details. The vertical dashed line corresponds to room temperature. The black lines represent VFT fits of the data for copolymers; see text for details. DC: Direct-current; VFT: vogel-fulcher-tammann.

amount of salt [Figure 2], leading to the currently proposed electrolyte concept with both mechanical robustness and conductivity levels relevant for battery technologies. To quantify the conductivity changes induced by the salt addition, the temperature dependences of  $\sigma_{DC}$  of Na and Li copolymers included in Figure 2 have been interpolated with Vogel-Fulcher-Tammann (VFT) functions  $\sigma_{DC} = \sigma_{DC,0} \cdot \exp[-D/(T-T_0)]$ , and the corresponding results of  $\sigma_{DC,0}$ ,  $D$ , and  $T_0$  parameters are included in Table 1. These data revealed that only copolymers with Li without salt have significantly higher  $T_0$  and probably higher glass transition temperatures. Adding salt strongly increases conductivity essentially without change of  $T_0$  in the case of Na-based copolymer [Figure 2].

By dissolving salt in the system, one expects that the added mobile anions will show some impact on the cation transport number,  $t_{+}$ . To access this parameter, two procedures are usually employed for Li-containing electrolytes. One is the Bruce-Vincent method, in which a constant voltage is applied to a Li symmetric cell for measurements of the current due to the migration of  $\text{Li}^+$  cations only ( $I^+$ ) and of the total current involving both anions and cations<sup>[47]</sup>. Using these currents, the cation transport number is determined as

$$t_{+,I} = \frac{I^+}{I^+ + I^-} \quad (1)$$

Employing this method to our Li electrolyte [Supplementary Figures 4 and 5] we obtained a  $t_{+,I}$  value of 0.4.



**Table 1. VFT parameters characterizing the temperature dependence of conductivity for the Na and Li copolymers with no salt and with salt**

Material	$\sigma_{DC,0}$ (S/cm)	$D$ (K)	$T_0$ (K)
Na no salt	0.010	1302	157
Li no salt	0.028	1035	185
Na with salt	0.188	1025	164
Li with salt	0.129	1012	162

VFT: Vogel-fulcher-tammann.

The second approach relies on knowledge of number densities and diffusion coefficients of cations and anions<sup>[48]</sup>, which is expressed as

$$t_{+,D} = \frac{n^+ D^+}{(n^+ D^+ + n^- D^-)} \quad (2)$$

For employing this second procedure we measured  $D^+$  and  $D^-$  corresponding to Li and TFSI ions, respectively, using NMR and their corresponding values are included in Figure 3. Interestingly, despite its significantly larger ion size, the diffusion coefficient of TFSI<sup>-</sup> is approximately twice larger than that of Li<sup>+</sup>. A possible reason for this behavior is that polymerized anionic groups slow down cations more strongly than anions. Using the experimentally probed diffusivities and the total number densities of mobile (excluding covalently bonded) ions, Eq. (2) yields a  $t_{+,D}$  value of 0.5.

We note that both definitions (for  $t_{+,I}$  and  $t_{+,D}$ ) are considered to be equivalent and rely on the validity of Nernst-Einstein relation; i.e., all ion-ion correlations are neglected<sup>[44,49]</sup>. However, in highly concentrated electrolytes in general, the Nernst-Einstein relation does not hold<sup>[50]</sup>. As demonstrated in Figure 3, for the present case, the estimations are based on this theoretical relation:

$$\sigma_{NE} = \frac{q^2 (n^+ D^+ + n^- D^-)}{k_B T} \quad (3)$$

which provides conductivity values larger than those of the experimentally probed ones. Such deviations between experimental and theoretical conductivities are usually quantified in terms of inverse Haven ratio (sometimes also called ionicity),  $H^{-1} \equiv \sigma_{DC}/\sigma_{NE}$ <sup>[14]</sup>. This parameter is a measure of the strength of ion cross-correlations which are known to suppress the macroscopic conductivity for liquid and polymeric electrolytes. Based on the data included in Figure 3, the investigated Li electrolyte displays  $H^{-1} \sim 0.5$ , a value similar to the one reported for ionic liquids<sup>[51]</sup> and indicating that ionic correlations suppress conductivity by about a factor of 2. We want to emphasize that the main suppression of ionic conductivity in these concentrated systems does not come from ion pairs, but rather from distinct cation-cation and anion-anion correlations<sup>[52,53]</sup>. This is clearly proven from analysis of the inverse Haven ratio in SICPs, where there are no mobile ion pairs and yet  $H^{-1}$  has much smaller values,  $\sim 0.1-0.01$ <sup>[14]</sup>. These ionic correlations are usually ascribed to momentum<sup>[54]</sup> or volume<sup>[55]</sup> conservation in the electrolytes, and are completely neglected in Eqs. 1 and 2. This makes estimates of  $t_+$  using Eqs. 1 and 2 qualitative rather than quantitative.

Before proceeding with battery testing, we also analyzed the role of the separator for the effective conductivity of the electrolyte. For this, we used a commercial Celgard separator [made of polypropylene (PP) and polyethylene (PE)] traditionally used for liquid-electrolyte batteries<sup>[56]</sup> and a PAN separator<sup>[57]</sup> (produced by electrospinning in our group). These have been impregnated with the Li-based precursor electrolyte, and their corresponding room-temperature conductivity spectra are included in Figure 4. These

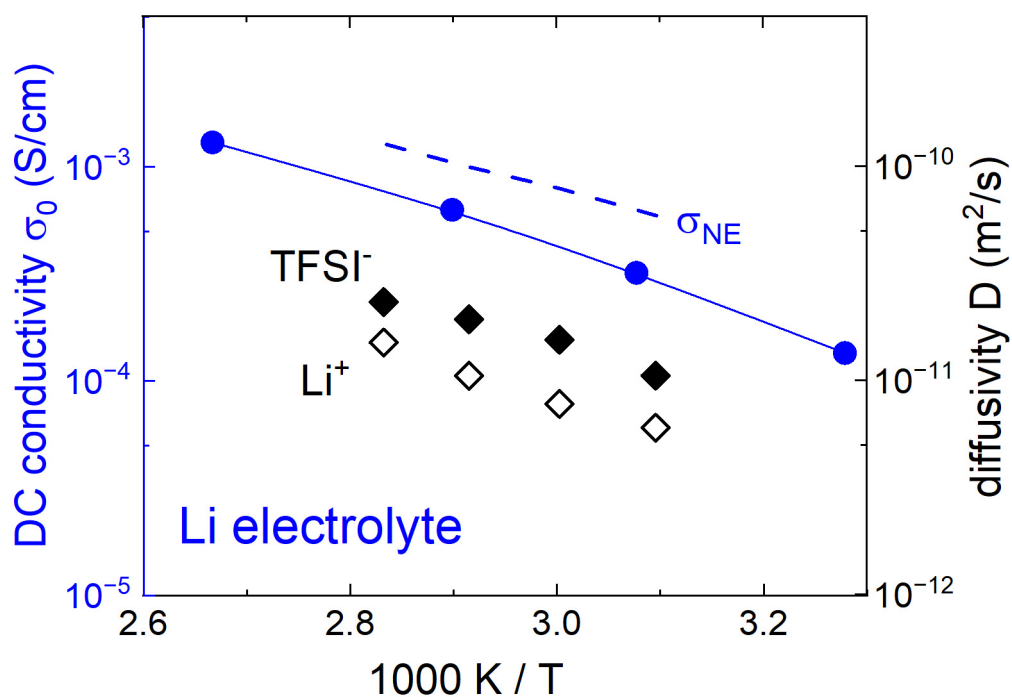


**Figure 3.** The temperature-dependent DC conductivity (blue dots) and the diffusivities of  $\text{Li}^+$  (black open diamonds) and  $\text{TFSI}^-$  (black filled diamonds) ions for the Li electrolyte. The blue dashed line presents the theoretically expected DC conductivity according to the Nernst-Einstein relation. DC: Direct-current; TFSI: trifluoromethanesulfonyl)imide.

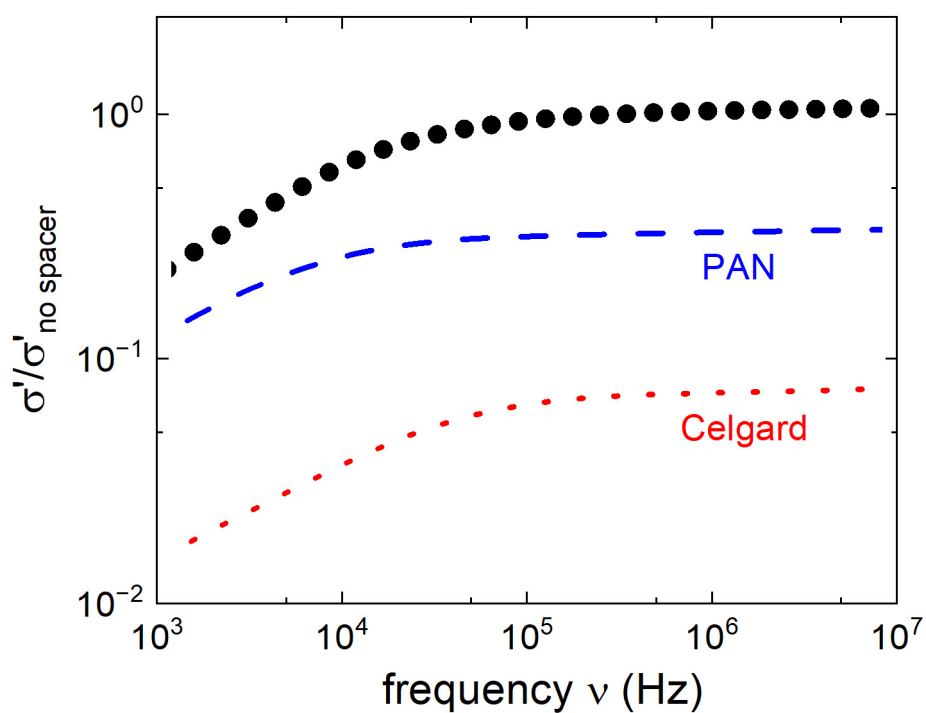


**Figure 4.** The room-temperature conductivity spectra of in situ polymerized and crosslinked polymer electrolytes in cell with Celgard separator (red dotted line) and PAN separator (blue dashed line) compared with the conductivity of the electrolyte without separators (black dots). PAN: Polyacrylonitrile.

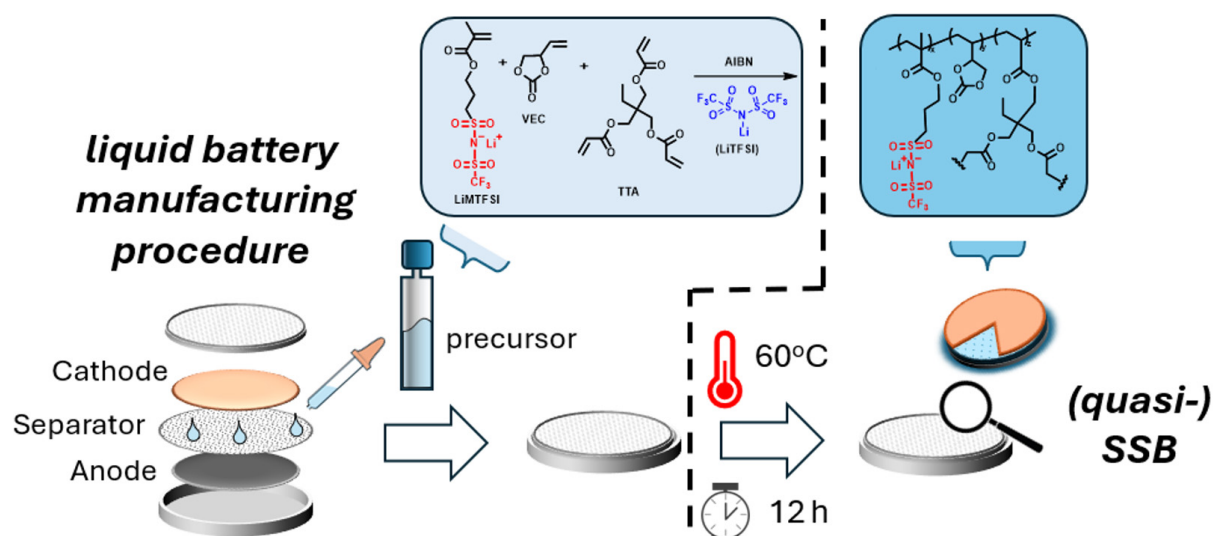
results reveal that Celgard reduces the conductivity of the electrolyte by about 15 times. Considering the nominal Celgard porosity of ~40%, this result demonstrates that this separator is poorly wetted by our electrolyte. In contrast, the PAN separator reduces the conductivity by a factor of 3 [Figure 4]. These results call for caution when choosing the battery separator, and prior analysis of their wettability by the chosen (liquid) electrolyte may be helpful in this regard.

### Battery implementation and testing

As schematically illustrated in Scheme 4, for preparing the battery cells, the precursor solution containing the two monomers, salt, initiator and crosslinkers is soaked into the separator and placed in direct contact with the electrodes. After the cell is sealed, the *in-situ* polymerization/crosslinking process is enabled within the battery by simply heating the latter at a given temperature for a given time. In this way, employing already existing technology for liquid electrolyte batteries<sup>[58]</sup>, (quasi) solid-state batteries (SSBs) can be developed with one additional heating step. No solvent is used in this process, just a mixture of monomers, initiators, crosslinkers and salt. Non-polymerized VEC monomers remain well-trapped in the formed crosslinked gel and will not leak.

The Li<sup>+</sup>-based copolymer was initially tested in Li<sup>+</sup>/Li symmetric cells using a 25-micron thick Celgard separator. The corresponding Nyquist plots recorded before and after the polarization of such a cell used for the previously mentioned Bruce-Vincent tests are shown in Figure 5A. They reveal a relatively small overall impedance of the Li electrolyte-electrodes system, below 350  $\Omega$ , demonstrating the formation of a low impedance EEI upon *in-situ* polymerization/crosslinking. These symmetric cells also display a stable voltage profile and low overpotential values of up to 1 mA/cm<sup>2</sup> current density [Figure 5B].

Long-term cycling of Li<sup>+</sup> electrolyte was also performed at 30 °C in real batteries incorporating a high-voltage (4.2 V) NMC-622 cathode, the Celgard separator, and a lithium metal anode. The results shown in Figure 6A demonstrate good capacity retention (~79%) during charging and discharging for 80 cycles at C/10 rate. The capacity value after 117 cycles was 101 mAh/g. The Coulombic efficiency was almost 100% in the entire measurement range. Including a similar type of results obtained for the non-crosslinked electrolyte, Figure 6A also demonstrates that *in-situ* crosslinking has a beneficial role in better preserving the capacity of the NMC-based batteries upon cycling. We note that these results have been obtained using Celgard as a separator, which, as previously shown, is poorly wetted by our electrolyte. In this regard, even better performance is expected for other types of separators. To test this hypothesis, the discharge capacity and Coulombic efficiency were also tested for a battery including a PAN separator and an LFP cathode. The latter has been used for presenting preliminary results with a focus on better understanding the electrolyte properties and improving the cycling performance of the cells, and future investigations will be considering NMC. The EIS plots before and after cycling as well as the voltage-capacity profile for the LFP cell have been included in the Supplementary Figures 6 and 7 (the EIS plots before and after curing have been included in the Supplementary Figures 8 and 9). The measured capacity is approximately 150 mAh/g over the measured 70 cycles at C/10 rate and the Coulombic efficiency is 100% [Figure 6A]. The capacity value is very close to the practical capacity of the LFP (165 mAh/g) and this performance improvement can be associated with the more porous separator that results in a better diffusion of the Li<sup>+</sup> ions through the PAN separator [Figure 3]. The Nyquist plot before and after cycling for the LFP cell is shown in Supplementary Figure 6. The bulk resistance of the cell did not change. The increase of the interfacial resistance after cycling can be attributed to the SEI formation, electrochemical reactions of the electrolyte and the electrodes or poor contact between the electrolyte and the active material. Additional studies are needed to better understand the mechanism for the increase of the resistance after cycling. The voltage versus specific capacity profile for the LFP cell in Figure 6A is shown in Supplementary Figure 7. The C-rate capability of the non-crosslinked NMC622 cell is presented in Supplementary Figure 10. The capacity fading becomes



**Scheme 4.** Depiction of the employed procedure for producing polymer-based quasi solid-state batteries by heating liquid-state manufactured batteries.

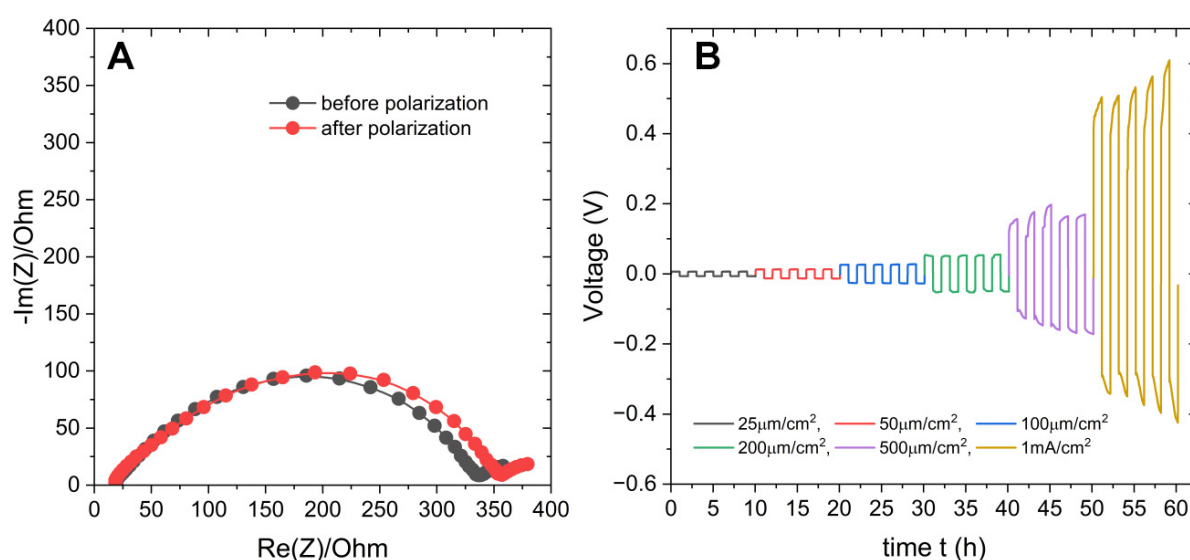


**Figure 5.** (A) Nyquist plots obtained before and after polarization for the calculation of the  $\text{Li}^+$  transport number; (B) Plating/stripping experiment at 30 °C shows stability of the cell up to 1 mA/ $\text{cm}^2$ . The half-cycle time is 1 h.

pronounced at C/3 and higher C-rates. Finally, the CV measurement of the  $\text{Li}^+$  electrolyte is shown in Figure 6B. These results indicate that the investigated material is stable in the entire voltage range without showing any spurious reactions due to the electrochemical degradation.

The good performance of the proposed polymer electrolyte in both symmetric cells and NMC/LFP batteries can be attributed to homogenous charge distribution during cycling due to *in-situ* polymerization and crosslinking. As the precursor can penetrate the electrode pores, after the polymerization it forms a uniformly charged network which helps Li to distribute homogeneously on the electrode. No signs of dendrite formation have been noted during these tests. Moreover, the decent transport numbers reduce cell polarization and enhance battery life by avoiding over-potential issues.

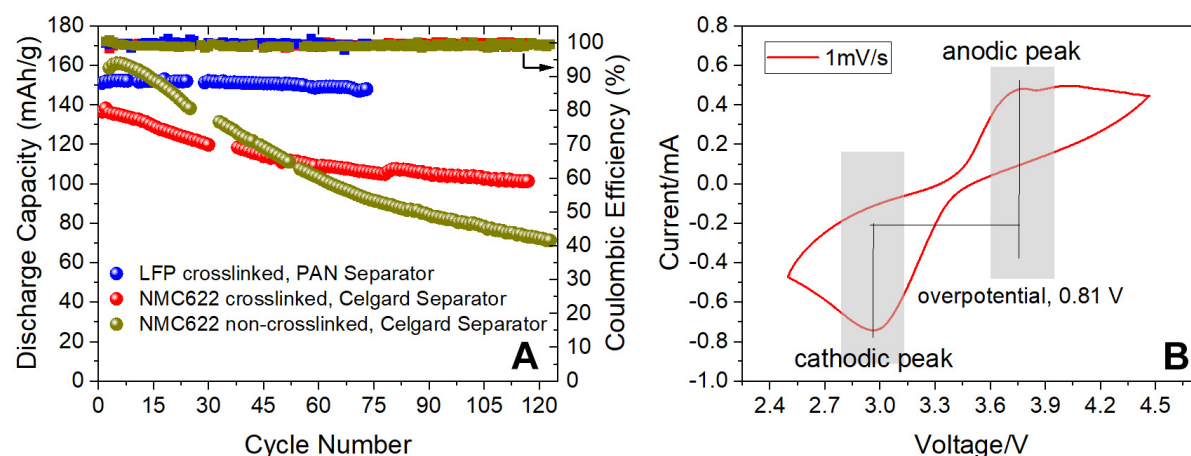


**Figure 6.** (A) Discharge capacity and Coulombic efficiency at 30 °C and C/10 rate for a high-voltage (4.2 V) NMC622 cathode with Celgard (2325) separator and an LFP cathode (3.7 V) with an electrospun PAN separator; A Li metal was used for the anode (B) CV plot for the electrolyte at 1 mV/s scan rate obtained for a cell with LFP cathode and Li metal anode. LFP: Lithium iron phosphate; PAN: polyacrylonitrile; CV: cyclic voltammetry.

## CONCLUSIONS

The present work introduces a concept of doped quasi single-ion conducting copolymers that can be polymerized and crosslinked *in-situ* and enabling (i) good adhesion with the electrodes, mitigating delamination and interfacial resistances; (ii) homogeneous distribution of charge carriers near the electrode surfaces to prevent dendrite formation; (iii) interchangeable Li and Na (and possibly other cations) transport using simple chemistry procedures, at variance with superionic ceramics where switching cations is obstructed by structural stability; (iv) relatively large Li and Na conductivities ( $\sim 0.1$  mS/cm at ambient conditions) and decent transport number ( $\sim 0.5$ ) which hampers polarization effects; and (v) mechanical robustness, with safety benefits in preventing electrolyte spilling upon battery damage. The proposed Li electrolyte demonstrated good performance in Li/Li symmetric cells, as well as in lithium metal cells with NMC or LFP cathode. Additionally, the proposed electrolyte concept is easy to implement with current battery technologies and provides a viable route for the design of high energy density safe polymer-based batteries capable of long duty cycles, in line with current global demands for energy storage.

## DECLARATIONS

### Authors' contributions

Provided research direction and funding support: Rahman, M. A.; Polizos, G.; Sokolov, A. P.; Gainaru, C.

Performed the dielectric measurements: Singh, H.; Beard, R.; Eberhard, R.

Analyzed the conductivity data: Singh, H.; Popov, I.

Performed the NMR investigations: Damron, J. T.

Performed chemical syntheses and characterizations: Danielson, M.; Rahman, M. A.

Performed battery cell assembly, electrochemical testing and data analysis: Polizos, G.; Shahriar, M.

All authors contributed to discussion of the results and manuscript writing.

### Availability of data and materials

Data are available from the corresponding authors upon reasonable request.

### Financial support and sponsorship

The authors acknowledge the support from Laboratory Directed Research and Development Fund, Oak Ridge National Laboratory, USA. Electrochemical measurements were supported by the DOE Vehicle

Technologies Office. Singh, H. acknowledges partial support from “Fast and Cooperative Ion Transport in Polymer-Based Materials (FaCT)”, an Energy Frontier Research Center funded by the U.S. Department of Energy, Office of Science, Basic Energy Sciences for its contribution to conductivity measurements, data analysis and interpretation.

### Conflicts of interest

All authors declared that there are no conflicts of interest.

### Ethical approval and consent to participate

Not applicable.

### Consent for publication

Not applicable.

### Copyright

© The Author(s) 2025.

## REFERENCES

- Li, Y.; Wang, X.; Dong, S.; Chen, X.; Cui, G. Recent advances in non-aqueous electrolyte for rechargeable Li-O<sub>2</sub> batteries. *Adv. Energy. Mater.* **2016**, 6, 1600751. DOI
- Yang, Y.; Zhao, L.; Zhang, Y.; et al. Challenges and prospects of low-temperature rechargeable batteries: electrolytes, interfaces, and electrodes. *Adv. Sci.* **2024**, 11, 2410318. DOI
- Angell, C. A. Fast ion motion in glassy and amorphous materials. *Solid. State. Ionics.* **1983**, 9-10, 3-16. DOI
- Ma, M.; Zhang, M.; Jiang, B.; Du, Y.; Hu, B.; Sun, C. A review of all-solid-state electrolytes for lithium batteries: high-voltage cathode materials, solid-state electrolytes and electrode-electrolyte interfaces. *Mater. Chem. Front.* **2023**, 7, 1268-97. DOI
- Muldoon, J.; Bucur, C. B.; Boaretto, N.; Gregory, T.; di, N. V. Polymers: opening doors to future batteries. *Polymer. Reviews.* **2015**, 55, 208-46. DOI
- Yi, J.; Guo, S.; He, P.; Zhou, H. Status and prospects of polymer electrolytes for solid-state Li-O<sub>2</sub> (air) batteries. *Energy. Environ. Sci.* **2017**, 10, 860-84. DOI
- Lee, M. J.; Han, J.; Lee, K.; et al. Elastomeric electrolytes for high-energy solid-state lithium batteries. *Nature* **2022**, 601, 217-22. DOI
- Hu, P.; Chai, J.; Duan, Y.; Liu, Z.; Cui, G.; Chen, L. Progress in nitrile-based polymer electrolytes for high performance lithium batteries. *J. Mater. Chem. A.* **2016**, 4, 10070-83. DOI
- Stacy, E. W.; Gainaru, C. P.; Gobet, M.; et al. Fundamental limitations of ionic conductivity in polymerized Ionic Liquids. *Macromolecules* **2018**, 51, 8637-45. DOI
- Edman, L.; Doeffer, M. M.; Ferry, A.; Kerr, J.; De, J. L. C. Transport properties of the solid polymer electrolyte system P(EO)<sub>n</sub> LiTFSI. *J. Phys. Chem. B.* **2000**, 104, 3476-80. DOI
- Mecerreyes, D. Polymeric ionic liquids: Broadening the properties and applications of polyelectrolytes. *Prog. Polym. Sci.* **2011**, 36, 1629-48. DOI
- Eftekhari, A.; Saito, T. Synthesis and properties of polymerized ionic liquids. *Eur. Polym. J.* **2017**, 90, 245-72. DOI
- Zhu, J.; Zhang, Z.; Zhao, S.; Westover, A. S.; Belharouak, I.; Cao, P. Single-ion conducting polymer electrolytes for solid-state lithium-metal batteries: design, performance, and challenges. *Adv. Energy. Mater.* **2021**, 11, 2003836. DOI
- Gainaru, C.; Stacy, E. W.; Bocharova, V.; et al. Mechanism of conductivity relaxation in liquid and polymeric electrolytes: direct link between conductivity and diffusivity. *J. Phys. Chem. B.* **2016**, 120, 11074-83. DOI
- Fan, F.; Wang, W.; Holt, A. P.; et al. Effect of molecular weight on the ion transport mechanism in polymerized ionic liquids. *Macromolecules* **2016**, 49, 4557-70. DOI
- Bae, J.; Oh, S.; Lee, B.; et al. High-performance, printable quasi-solid-state electrolytes toward all 3D direct ink writing of shape-versatile Li-ion batteries. *Energy. Storage. Mater.* **2023**, 57, 277-88. DOI
- Ahmed, F.; Choi, I.; Rahman, M. M.; et al. Remarkable conductivity of a self-healing single-ion conducting polymer electrolyte, poly(ethylene-co-acrylic lithium (fluoro sulfonyl)imide), for all-solid-state Li-ion batteries. *ACS. Appl. Mater. Interfaces.* **2019**, 11, 34930-8. DOI
- Luo, Y.; Gao, L.; Kang, W. A new review of single-ion conducting polymer electrolytes in the light of ion transport mechanisms. *J. Energy. Chem.* **2024**, 89, 543-56. DOI
- Pozyczka, K.; Marzantowicz, M.; Dygas, J.; Krok, F. Ionic conductivity and lithium transference number of poly(ethylene oxide):LiTFSI system. *Electrochim. Acta.* **2017**, 227, 127-35. DOI



20. Song, J.; Wang, Y.; Wan, C. Review of gel-type polymer electrolytes for lithium-ion batteries. *J. Power. Sources.* **1999**, *77*, 183-97. DOI
21. Lehmann, M. L.; Yang, G.; Gilmer, D.; et al. Tailored crosslinking of Poly(ethylene oxide) enables mechanical robustness and improved sodium-ion conductivity. *Energy. Storage. Mater.* **2019**, *21*, 85-96. DOI
22. Li, L.; Li, S.; Lu, Y. Suppression of dendritic lithium growth in lithium metal-based batteries. *Chem. Commun.* **2018**, *54*, 6648-61. DOI
23. Lee, H. G.; Kim, S. Y.; Lee, J. S. Dynamic observation of dendrite growth on lithium metal anode during battery charging/discharging cycles. *npj. Comput. Mater.* **2022**, *8*, 103. DOI
24. Maity, A.; Svirinovsky-Arbeli, A.; Buganim, Y.; Oppenheim, C.; Leskes, M. Tracking dendrites and solid electrolyte interphase formation with dynamic nuclear polarization-NMR spectroscopy. *Nat. Commun.* **2024**, *15*, 9956. DOI PubMed PMC
25. Bocharova, V.; Sokolov, A. P. Perspectives for polymer electrolytes: a view from fundamentals of ionic conductivity. *Macromolecules* **2020**, *53*, 4141-57. DOI
26. Shan, C.; Wang, Y.; Liang, M.; et al. A comprehensive review of single ion-conducting polymer electrolytes as a key component of lithium metal batteries: From structural design to applications. *Energy. Storage. Mater.* **2023**, *63*, 102955. DOI
27. Ghorbanzade, P.; Loaiza, L. C.; Johansson, P. Plasticized and salt-doped single-ion conducting polymer electrolytes for lithium batteries. *RSC. Adv.* **2022**, *12*, 18164-7. DOI PubMed PMC
28. Swift, M. W.; Jagad, H.; Park, J.; Qie, Y.; Wu, Y.; Qi, Y. Predicting low-impedance interfaces for solid-state batteries. *Curr. Opin. Solid. State. Mater. Sci.* **2022**, *26*, 100990. DOI
29. Wang, H.; Yu, Z.; Kong, X.; et al. Liquid electrolyte: the nexus of practical lithium metal batteries. *Joule* **2022**, *6*, 588-616. DOI
30. Guan, X.; Wu, Q.; Zhang, X.; Guo, X.; Li, C.; Xu, J. In-situ crosslinked single ion gel polymer electrolyte with superior performances for lithium metal batteries. *Chem. Eng. J.* **2020**, *382*, 122935. DOI
31. He, P.; Chen, S.; Choi, Y. Y.; Myung, N. V.; Nykaza, J. R.; Schaefer, J. L. In-situ crosslinked gel polymer electrolytes based on ionic monomers as charge carriers for lithium-ion batteries. *ECS. Adv.* **2024**, *3*, 010504. DOI
32. Shan, X.; Morey, M.; Li, Z.; et al. A polymer electrolyte with high cationic transport number for safe and stable solid Li-metal batteries. *ACS. Energy. Lett.* **2022**, *7*, 4342-51. DOI
33. Xiao, G.; Xu, H.; Bai, C.; Liu, M.; He, Y. Progress and perspectives of in situ polymerization method for lithium-based batteries. *Interdiscip. Mater.* **2023**, *2*, 609-34. DOI
34. Zhang, Q.; Liu, S.; Lin, Z.; et al. Highly safe and cyclable Li-metal batteries with vinyl ethylene carbonate electrolyte. *Nano. Energy.* **2020**, *74*, 104860. DOI
35. Devaux, D.; Liénafa, L.; Beaudoin, E.; et al. Comparison of single-ion-conductor block-copolymer electrolytes with polystyrene-TFPI and polymethacrylate-TFPI structural blocks. *Electrochim. Acta.* **2018**, *269*, 250-61. DOI
36. Au, H.; Crespo-ribadeneyra, M.; Titirici, M. Beyond Li-ion batteries: performance, materials diversification, and sustainability. *One. Earth.* **2022**, *5*, 207-11. DOI
37. Gao, Y.; Pan, Z.; Sun, J.; Liu, Z.; Wang, J. High-energy batteries: beyond lithium-ion and their long road to commercialisation. *Nano-Micro. Lett.* **2022**, *14*, 94. DOI PubMed PMC
38. Tian, Y.; Zeng, G.; Rutt, A.; et al. Promises and challenges of next-generation “beyond li-ion” batteries for electric vehicles and grid decarbonization. *Chem. Rev.* **2021**, *121*, 1623-69. DOI
39. Vedhanarayanan, B.; Seetha, L. K. C. Beyond lithium-ion: emerging frontiers in next-generation battery technologies. *Front. Batter. Electrochem.* **2024**, *3*, 1377192. DOI
40. Zhou, D.; Shanmukaraj, D.; Tkacheva, A.; Armand, M.; Wang, G. Polymer electrolytes for lithium-based batteries: advances and prospects. *Chem* **2019**, *5*, 2326-52. DOI
41. Barbosa, J. C.; Gonçalves, R.; Costa, C. M.; Lanceros-Méndez, S. Toward sustainable solid polymer electrolytes for lithium-ion batteries. *ACS. Omega.* **2022**, *7*, 14457-64. DOI PubMed PMC
42. Mu, J.; Liao, S.; Shi, L.; et al. Solid-state polymer electrolytes in lithium batteries: latest progress and perspective. *Polym. Chem.* **2024**, *15*, 473-99. DOI
43. Song, Z.; Chen, F.; Martínez-Ibañez, M.; et al. A reflection on polymer electrolytes for solid-state lithium metal batteries. *Nat. Commun.* **2023**, *14*, 4884. DOI PubMed PMC
44. Dyre, J. C.; Maass, P.; Roling, B.; Sidebottom, D. L. Fundamental questions relating to ion conduction in disordered solids. *Rep. Prog. Phys.* **2009**, *72*, 046501. DOI
45. Ishai, P. B.; Talary, M. S.; Caduff, A.; Levy, E.; Feldman, Y. Electrode polarization in dielectric measurements: a review. *Meas. Sci. Technol.* **2013**, *24*, 102001. DOI
46. Gainaru, C.; Kumar, R.; Popov, I.; et al. Mechanisms controlling the energy barrier for ion hopping in polymer electrolytes. *Macromolecules* **2023**, *56*, 6051-9. DOI
47. Evans, J.; Vincent, C. A.; Bruce, P. G. Electrochemical measurement of transference numbers in polymer electrolytes. *Polymer* **1987**, *28*, 2324-8. DOI
48. Fong, K. D.; Self, J.; Diederichsen, K. M.; Wood, B. M.; McCloskey, B. D.; Persson, K. A. Ion transport and the true transference number in nonaqueous polyelectrolyte solutions for lithium ion batteries. *ACS. Cent. Sci.* **2019**, *5*, 1250-60. DOI PubMed PMC
49. Maass, P.; Meyer, M.; Bunde, A. Nonstandard relaxation behavior in ionically conducting materials. *Phys. Rev. B.* **1995**, *51*, 8164. DOI

50. Murch, G. The Haven ratio in fast ionic conductors. *Solid. State. Ionics*. **1982**, *7*, 177-98. [DOI](#)
51. Sangoro, J. R.; Kremer, F. Charge transport and glassy dynamics in ionic liquids. *Acc. Chem. Res.* **2012**, *45*, 525-32. [DOI](#) [PubMed](#)
52. Vargas-barbosa, N. M.; Roling, B. Dynamic ion correlations in solid and liquid electrolytes: how do they affect charge and mass transport? *ChemElectroChem* **2020**, *7*, 367-85. [DOI](#)
53. Pothmann, T.; Middendorf, M.; Gerken, C.; Nürnberg, P.; Schönhoff, M.; Roling, B. Overdetermination method for accurate dynamic ion correlations in highly concentrated electrolytes. *Faraday. Discuss.* **2024**, *253*, 100-17. [DOI](#) [PubMed](#)
54. Ahmed, M. D.; Zhu, Z.; Khamzin, A.; Paddison, S. J.; Sokolov, A. P.; Popov, I. Effect of ion mass on dynamic correlations in ionic liquids. *J. Phys. Chem. B*. **2023**, *127*, 10411-21. [DOI](#) [PubMed](#)
55. Lorenz, M.; Kilchert, F.; Nürnberg, P.; et al. Local volume conservation in concentrated electrolytes is governing charge transport in electric fields. *J. Phys. Chem. Lett.* **2022**, *13*, 8761-7. [DOI](#)
56. Arora, P.; Zhang, Z. J. Battery separators. *Chem. Rev.* **2004**, *104*, 4419-62. [DOI](#) [PubMed](#)
57. Sheng, J.; Zhang, Q.; Sun, C.; et al. Crosslinked nanofiber-reinforced solid-state electrolytes with polysulfide fixation effect towards high safety flexible lithium-sulfur batteries. *Adv. Funct. Mater.* **2022**, *32*, 2203272. [DOI](#)
58. Knoche, T.; Surek, F.; Reinhart, G. A process model for the electrolyte filling of lithium-ion batteries. *Procedia. CIRP*. **2016**, *41*, 405-10. [DOI](#)